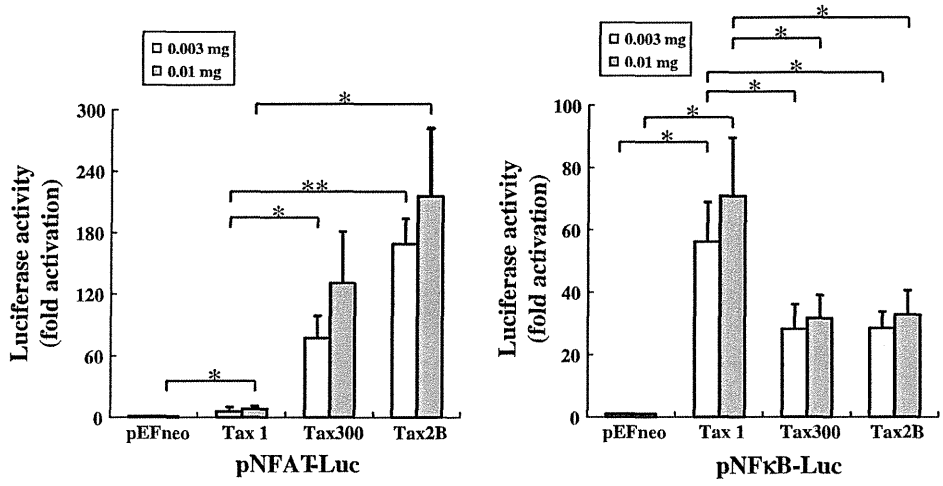


**Fig. 4** Tax2B activates both NFAT and NF-κB in a T cell line. Jurkat cells ($2 \times 10^5$ cells/1.0 ml/well) in a 12-well plate were co-transfected with the Tax expression plasmid and pGK/β-gal, together with either pNFAT-Luc or κB-Luc, using TransFectin. At 48 h after transfection, the luciferase and β-galactosidase activities in the lysates were determined using a luminometer. The activity of luciferase was normalized to that of β-galactosidase, and the fold activations were calculated as the ratio to that of the control transfection with the pEFneo plasmid. The data shown are the averages of three independent experiments with standard deviations. *One asterisk* and *two asterisks* indicate significant differences ($p < 0.05$) and ($p < 0.01$) by the unpaired student's *t* test, respectively

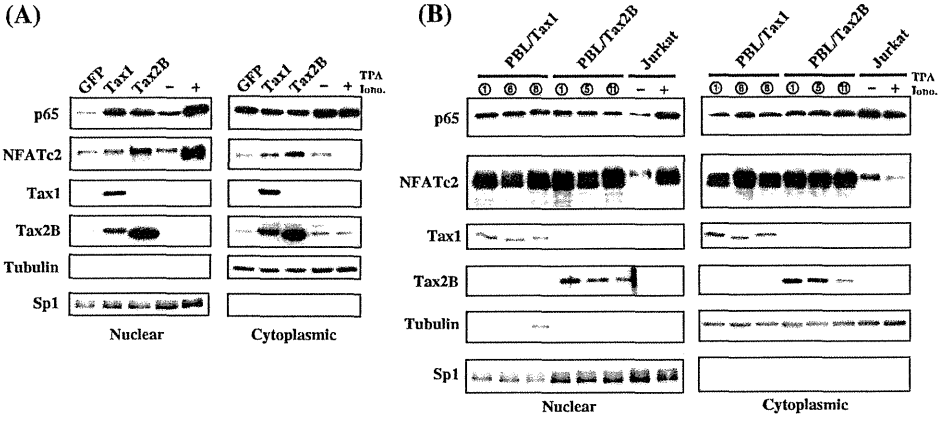


**Fig. 5** Tax2B induces the nuclear translocation of NFATc2 and p65 in T cells. **a**, **b** Jurkat cells ($4 \times 10^5$ cells) were infected with bicistranic Tax1-EGFP lentivirus, Tax2B-EGFP lentivirus or the control virus in 6-well plate and were cultured for 48 h. Jurkat cells ($2 \times 10^6$ cells) were treated with 20 ng/ml TPA and 1 μM ionomycin for 60 min. Cytoplasmic and nuclear fractions from the infected Jurkat cells (**a**) and Tax-immortalized cells (**b**) were analyzed by a Western blotting analysis using anti-p65, anti-NFATc2, anti-Tax1, anti-Tax2B, anti-Tubulin, and anti-Sp1 antibodies. Tubulin and Sp1 were used as marker proteins that localize in the cytoplasm and the nucleus, respectively

were also equivalent to that of stimulated Jurkat, thus suggesting that Tax1- and Tax2B-immortalized cells have augmented p65- and NFATc2-dependent transcriptional activities. However, it should be noted that the high levels of nuclear NFATc2 in Tax1-immortalized T cells were unexpected, as Tax1 showed a much lower NFAT transcriptional activity than that of Tax2B (Figs. 4b, 5a). Collectively, these results suggested that Tax1- and Tax2B-immortalized T cells have equivalent activations of NF-κB p65 and NFATc2, which did not support the possibility that NFAT contributes to the distinct immortalization activity of Tax2B versus Tax1.

## Discussion

In this study, we demonstrated that the HTLV-2b Tax2B protein has an immortalizing activity in human T cells within PBMCs, and such cells could be long-term cultured for at least 3 months (Fig. 2). A previous study showed that

*tax2*-inactivated HTLV-2 does not immortalize human T cells [25]. Taken together, these findings indicate that Tax2 is a crucial factor required for the immortalization of HTLV-2-infected T cells, thereby leading to persistent infection.

HTLV-2 and HTLV-1 preferentially immortalize $CD8^+$ T cells and $CD4^+$ T cells, respectively, in vitro [26]. Nevertheless, Tax2B selectively immortalized $CD4^+$ T cells, but not $CD8^+$ T cells, in this study (Fig. 3). These results indicate that Tax2 is not a determinant for the immortalization tropism of HTLV-2. Indeed, the chimeric virus composed of HTLV-2 and HTLV-1 showed that the *envelope* gene, but not *tax2*, is a determinant for the selective immortalization of $CD8^+$ T cells by HTLV-2 [27].

The immortalization activity of Tax2B on human T cells was much more efficient than that of Tax1 (Fig. 2). A microscopic examination revealed that Tax1 and Tax2 initially induce the outgrowth of PBMCs for 1 week. Thereafter, while the Tax2-transduced cells continue to grow, Tax1-transduced cells stop growing for several weeks, and then some cells start to regrow. The overexpression of Tax1 in several cell types, including a T cell line, was shown to induce senescence and/or cell cycle arrest [28, 29]. Therefore, such growth inhibitory activity of Tax1 might explain why Tax1-infected PBMCs stop growing for a while in culture. Tax2 might not have these growth inhibitory activities, thereby inducing greater immortalization activity in T cells than Tax1. It should be noted that HTLV-1 HBZ, which shows an oncogenic activity in transgenic mice, alleviates the growth inhibitory activity of Tax1 [10, 29]. Collectively, we herein present a hypothesis that Tax2 alone is sufficient to immortalize T cells by HTLV-2, whereas both Tax1 and HBZ are required to efficiently immortalize T cells by HTLV-1.

The same set of the lentiviruses used here previously showed that Tax1 induces IL-2-independent growth transformation to the originally IL-2-dependent T cell line, CTLL-2, and that the activity was much higher than that of Tax2B and Tax300 [16, 20]. Therefore, it was intriguing that Tax2 and Tax1 have such distinct activities to T cells in the absence and presence of IL-2, despite the fact that they originated from the common ancestor virus. One possible scenario is that Tax2 in the context of HTLV-2 has evolved to immortalize T cells in the presence of a relatively high amount of IL-2, whereas Tax1 in the context of HTLV-1 has evolved to do so in a relatively low amount of IL-2 [30]. A further analysis, however, will be required to establish this hypothesis and to determine how these differences are associated with the leukemogenic activity of HTLV-1.

In addition to NF-κB and NFAT, Tax1 activates the transcription of several cellular genes through the transcription factor CREB, and Rosin et al. [31] presented an evidence that the activation of CREB pathway by Tax1 is important for the immortalization of primary human T cells by Tax1. However, the CREB pathway is unlikely to be a main factor for the reduced immortalization activity of Tax1 relative to Tax2B, as Tax1 and Tax2B showed equivalent CREB activities in a luciferase reporter assay [18]. It should be noted that Tax1 and Tax300, but not Tax2B, have a PDZ domain binding motif (PBM) at their C-terminus (Fig. 4a), and this motif is critical for the high transforming activity of Tax1 to CTLL-2 [32]. However, Xie et al. [33] showed that the deletion of PBM in recombinant HTLV-1 minimally affects immortalization activity to human T cells in the presence of IL-2. Therefore, this motif is unlikely to be responsible for distinct immortalization activities of Tax1 and Tax2B in human T cells. Tax1 and Tax2B have other distinctions from PBM. For instance, Tax1 but neither Tax2B nor Tax300 activates the non-canonical NF-κB2 pathway, which also plays a critical role in the high transforming activity toward CTLL-2 [16, 17]. Therefore, precise comparisons of Tax1 and Tax2B including these differences are required to identify the function(s) responsible for immortalization of human T cells as well as the pathogenesis.

**Acknowledgments** We would like to thank Dr. Hiroyuki Miyoshi at RIKEN Tsukuba Institute for providing the lentivirus plasmids, and Dr. Renaud Mahieux and Dr. William Hall for providing the anti-Tax2 antibody and *tax2B* gene, respectively. We also wish to thank the Takeda Pharmaceutical Company for providing recombinant human IL-2. We would like to express our gratitude to Misako Tobimatsu for the excellent technical assistance. This study was supported in part by a Grant-in-Aid for Scientific Research on Priority Areas and for Scientific Research (C) of Japan, as well as a Grant for the Promotion of Niigata University Research Projects.

## References

1. T. Uchiyama, J. Yodoi, K. Sagawa, K. Takatsuki, H. Uchino, Blood **50**(3), 481–492 (1977)
2. B.J. Poiesz, F.W. Ruscetti, A.F. Gazdar, P.A. Bunn, J.D. Minna, R.C. Gallo, Proc Natl Acad Sci USA **77**(12), 7415–7419 (1980)
3. Y. Hinuma, H. Komoda, T. Chosa, T. Kondo, M. Kohakura, T. Takenaka, M. Kikuchi, M. Ichimaru, K. Yunoki, I. Sato, R. Matsuo, Y. Takiuchi, H. Uchino, M. Hanaoka, Int. J. Cancer **29**(6), 631–635 (1982)
4. M. Matsuoka, K. T. Jeang, Oncogene 30(12), 1379–1389 (2011)
5. I. Miyoshi, I. Kubonishi, S. Yoshimoto, T. Akagi, Y. Ohtsuki, Y. Shiraishi, K. Nagata, Y. Hinuma, Nature **294**(5843), 770–771 (1981)
6. W.W. Hall, M. Fujii, Oncogene **24**(39), 5965–5975 (2005)
7. P. Miyazato, J. Yasunaga, Y. Taniguchi, Y. Koyanagi, H. Mitsuya, M. Matsuoka, J. Virol. **80**(21), 10683–10691 (2006)
8. H. Hasegawa, H. Sawa, M.J. Lewis, Y. Orba, N. Sheehy, Y. Yamamoto, T. Ichinohe, Y. Tsunetsugu-Yokota, H. Katano, H. Takahashi, J. Matsuda, T. Sata, T. Kurata, K. Nagashima, W.W. Hall, Nat. Med. **12**(4), 466–472 (2006)
9. T. Ohsugi, T. Kumasaka, S. Okada, T. Urano, Nat. Med. **13**(5), 527–528 (2007)

10. Y. Satou, J. Yasunaga, T. Zhao, M. Yoshida, P. Miyazato, K. Takai, K. Shimizu, K. Ohshima, P.L. Green, N. Ohkura, T. Yamaguchi, M. Ono, S. Sakaguchi, M. Matsuoka, PLoS Pathog. **7**(2), e1001274 (2011)
11. M.D. Robek, L. Ratner, J. Virol. **73**(6), 4856–4865 (1999)
12. R. Grassmann, S. Berchtold, I. Radant, M. Alt, B. Fleckenstein, J.G. Sodroski, W.A. Haseltine, U. Ramstedt, J. Virol. **66**(7), 4570–4575 (1992)
13. T. Akagi, K. Shimotohno, J. Virol. **67**(3), 1211–1217 (1993)
14. V.S. Kalyanaraman, M.G. Sarngadharan, M. Robert-Guroff, I. Miyoshi, D. Golde, R.C. Gallo, Science **218**(4572), 571–573 (1982)
15. M.J. Lewis, P. Novoa, R. Ishak, M. Ishak, M. Salemi, A.M. Vandamme, M.H. Kaplan, W.W. Hall, Virology **271**(1), 142–154 (2000)
16. M. Higuchi, C. Tsubata, R. Kondo, S. Yoshida, M. Takahashi, M. Oie, Y. Tanaka, R. Mahieux, M. Matsuoka, M. Fujii, J. Virol. **81**(21), 11900–11907 (2007)
17. T. Shoji, M. Higuchi, R. Kondo, M. Takahashi, M. Oie, Y. Tanaka, Y. Aoyagi, M. Fujii, Retrovirology **6**, 83 (2009)
18. A. Niinuma, M. Higuchi, M. Takahashi, M. Oie, Y. Tanaka, F. Gejyo, N. Tanaka, K. Sugamura, L. Xie, P.L. Green, M. Fujii, J. Virol. **79**(18), 11925–11934 (2005)
19. J.P. Northrop, K.S. Ullman, G.R. Crabtree, J. Biol. Chem. **268**(4), 2917–2923 (1993)
20. K. Endo, A. Hirata, K. Iwai, M. Sakurai, M. Fukushi, M. Oie, M. Higuchi, W.W. Hall, F. Gejyo, M. Fujii, J. Virol. **76**(6), 2648–2653 (2002)
21. Y. Tanaka, A. Yoshida, H. Tozawa, H. Shida, H. Nyunoya, K. Shimotohno, Int. J. Cancer **48**(4), 623–630 (1991)
22. L. Meertens, S. Chevalier, R. Weil, A. Gessain, R. Mahieux, J. Biol. Chem. **279**(41), 43307–43320 (2004)
23. T. Akagi, H. Ono, H. Nyunoya, K. Shimotohno, Oncogene **14**(17), 2071–2078 (1997)
24. S.C. Sun, S. Yamaoka, Oncogene **24**(39), 5952–5964 (2005)
25. T.M. Ross, S.M. Pettiford, P.L. Green, J. Virol. **70**(8), 5194–5202 (1996)
26. J. Ye, L. Xie, P.L. Green, J. Virol. **77**(14), 7728–7735 (2003)
27. L. Xie, P.L. Green, J. Virol. **79**(23), 14536–14545 (2005)
28. M. Liu, L. Yang, L. Zhang, B. Liu, R. Merling, Z. Xia, C.Z. Giam, J. Virol. **82**(17), 8442–8455 (2008)
29. H. Zhi, L. Yang, Y.L. Kuo, Y.K. Ho, H.M. Shih, C.Z. Giam, PLoS Pathog. **7**(4), e1002025 (2011)
30. M. Higuchi, M. Fujii, Retrovirology **6**, 117 (2009)
31. O. Rosin, C. Koch, I. Schmitt, O.J. Semmes, K.T. Jeang, R. Grassmann, J. Biol. Chem. **273**(12), 6698–6703 (1998)
32. C. Tsubata, M. Higuchi, M. Takahashi, M. Oie, Y. Tanaka, F. Gejyo, M. Fujii, Retrovirology **2**, 46 (2005)
33. L. Xie, B. Yamamoto, A. Haoudi, O.J. Semmes, P.L. Green, Blood **107**(5), 1980–1988 (2006)
34. A. Hirata, M. Higuchi, A. Niinuma, M. Ohashi, M. Fukushi, M. Oie, T. Akiyama, Y. Tanaka, F. Gejyo, M. Fujii, Virology **318**(1), 327–336 (2004)

Surg Today
DOI 10.1007/s00595-012-0316-4

CASE REPORT

# Successful laparoscopic division of a patent ductus venosus: report of a case

**Yoshiaki Hara · Yoshinobu Sato · Satoshi Yamamoto · Hiroshi Oya · Masato Igarashi · Satoshi Abe · Hidenaka Kokai · Kohei Miura · Takeshi Suda · Minoru Nomoto · Yutaka Aoyagi · Katsuyoshi Hatakeyama**

Received: 14 May 2011 / Accepted: 15 December 2011


**Abstract** Patent ductus venosus (PDV) is a rare condition of a congenital portosystemic shunt from the umbilical vein to the inferior vena cava. This report presents the case of an adult patient with PDV, who was successfully treated with laparoscopic shunt division. A 69-year-old male was referred with hepatic encephalopathy. Contrast-enhanced CT revealed a large connection between the left portal vein and the inferior vena cava, which was diagnosed as PDV. The safety of a shunt disconnection was confirmed using a temporary balloon occlusion test for the shunt, and the shunt division was performed laparoscopically. The shunt was carefully separated from the liver parenchyma with relative ease, and then divided using a vascular stapler. Portal flow was markedly increased after the operation, and the liver function of the patient improved over the 3-month period after surgery. Although careful interventional evaluation for portal flow is absolutely imperative prior to surgery, a minimally invasive laparoscopic approach can be safely used for treating PDV.

**Keywords** Patent ductus venosus · Laparoscopic surgery · Portosystemic shunt division

Y. Hara (✉) · Y. Sato · S. Yamamoto · H. Oya · H. Kokai · K. Miura · K. Hatakeyama
Division of Digestive and General Surgery, Niigata University Graduate School of Medical and Dental Sciences,
1-757 Asahimachi-dori, Chuo-ku, Niigata 951-8510, Japan
e-mail: yhara02@attglobal.net

M. Igarashi · S. Abe · T. Suda · M. Nomoto · Y. Aoyagi
Division of Gastroenterology and Hepatology,
Niigata University Graduate School of Medical and Dental Sciences, Niigata, Japan

## Introduction

Patent ductus venosus (PDV) is a rare condition of a congenital portosystemic shunt from the umbilical vein to the inferior vena cava (IVC), which is rarely seen in either children or adults. The symptoms of this disorder include encephalopathy, hyperammonemia, jaundice, and liver dysfunction. Reported treatments have included radiological occlusion, surgical ligation or banding under laparotomy, and liver transplantation, but the use of these procedures is controversial [1, 2]. This report presents the case of an adult patient with ductus venosus, which was successfully treated with laparoscopic shunt division.

## Case report

A 69-year-old male was referred with hepatic encephalopathy, following a 3-month history of tremor and disturbance of orientation. Although slightly elevated bilirubin had been detected for a long time, he had not undergone any further examination. Laboratory data showed hyperammonemia (113 μg/dl), mildly elevated bilirubin (4.8 mg/dl), and prolonged PT-INR (1.94). Contrast-enhanced abdominal CT confirmed a notable attenuation of the intrahepatic portal branches and a large connection between the umbilical part of the left branch of the portal vein and the IVC (Fig. 1a). An echogram also indicated diminished portal venous flow (Fig. 1b). A liver biopsy revealed sectional mild fibrosis and sinusoidal dilatation, which were thought to be due to decreased portal flow, no inflammatory change. Primary hepatic disorder was also excluded by a series of blood tests, and the patient was diagnosed as having patent ductus venosus.

Published online: 04 September 2012

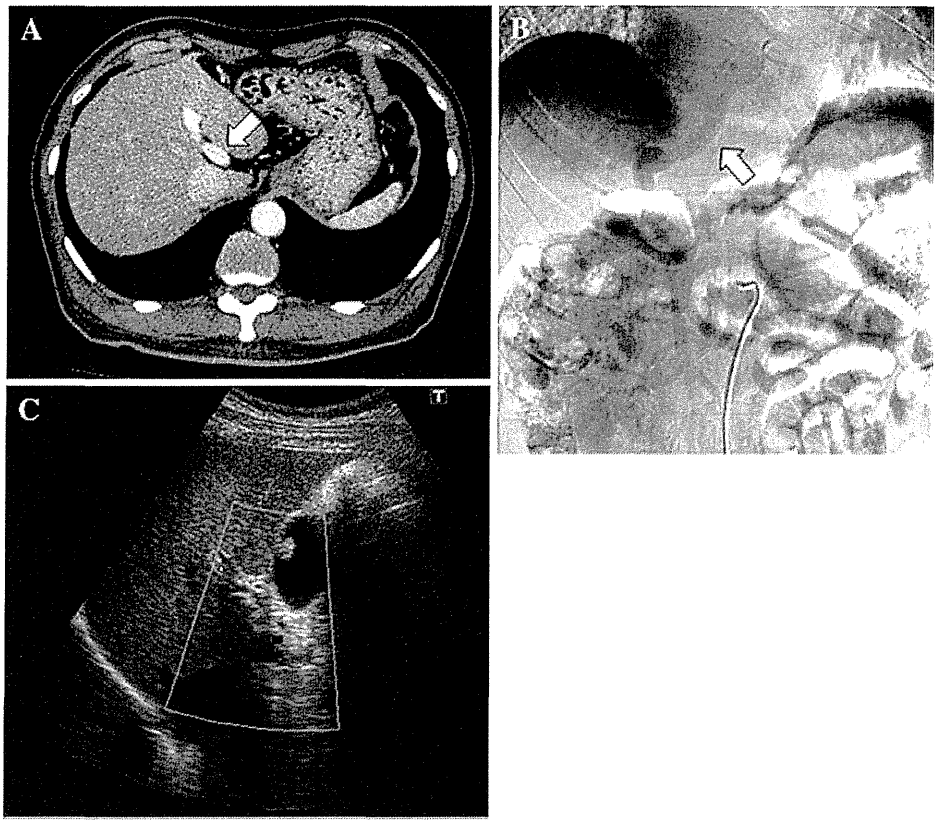


**Fig. 1** Enhanced CT (**a**) and portal venography (**b**) reveal an abnormal vein connecting the left portal vein to the inferior vena cava through the fissure of ligamentum venosum (*white arrow*). Doppler ultrasonography reveals decreased intrahepatic portal flow (**c**). A small polyp was also detected in the gall bladder

A balloon occlusion test for the shunt was performed using transcatheter venography to confirm the safety of shunt disconnection. Portal venography via the superior mesenteric artery found narrowing of the peripheral portal vein and an enlarged PDV between the left branch of the portal vein and the IVC (Fig. 1c). A 5-French balloon catheter was inserted from the right internal jugular vein into the ductus venosus via the IVC. Portal venous pressure was then measured before and after shunt occlusion by balloon inflation. The mean portal venous pressure (PVP) before shunt occlusion was 12.2 $cmH_2O$. Temporary balloon occlusion increased the PVP to 21.8 $cmH_2O$ and then it gradually decreased to 13.6 $cmH_2O$ during a 60-min occlusion, suggesting that shunt disconnection or occlusion could be safely performed. Radiological embolization carries the risk of coil migration due to the high flow and the large diameter of the shunt, and thus laparoscopic shunt division was performed.

The patient was placed under general anesthesia, and four trocars were introduced into the anterior abdominal wall (Fig. 2). The surgeon stood on the left side of the patient. The liver appeared non-cirrhotic but slightly fibrotic and hard with a rough surface. A cholecystectomy was performed prior to shunt disconnection, because the patient also had a cholecystic polyp. An additional trocar was introduced into the left side of the abdomen following

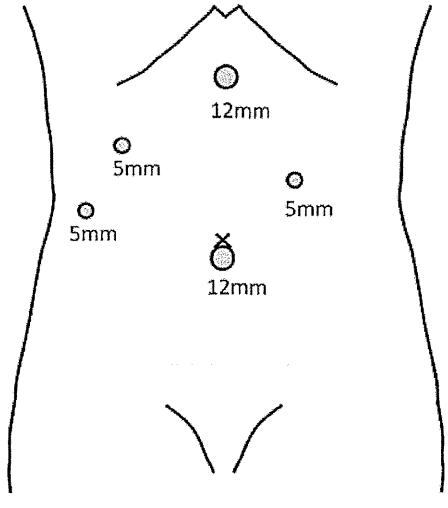


**Fig. 2** Sites of trocar placement. Cholecystectomy was first performed through four ports to remove a cholecystic polyp, then a left-side port was added and the PDV was divided

the cholecystectomy, and then the lesser omentum was dissected to exteriorize the Spiegel lobe. The PDV was detected as an enlarged vessel along the sulcus of the ligamentum venosum, on the anterior aspect of the Spiegel lobe (Fig. 3a). There was no collateral flow around the PDV, and the vessel was carefully separated from the liver

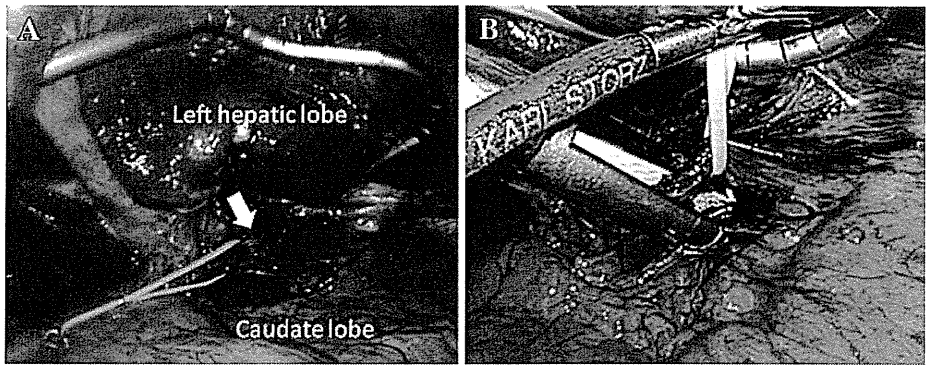


**Fig. 3** The enlarged vessel between the left portal vein and the inferior vena cava was separated (**a**) and divided using vascular stapler (**b**)

parenchyma with relative ease. The shunt was then divided at the proximal part close to the branching point from the left portal vein using a 60-mm Echelon stapler (Fig. 3b). The total duration of the operation was 183 min, including the time for the cholecystectomy, and the total blood loss was very low. Although the patient's post-operative condition was stable, a portal thrombus at the umbilical portion was detected by enhanced CT on day 6. Thrombolytic therapy was performed, and the thrombus almost disappeared within 1 month after surgery. A post-operative echogram indicated markedly increased blood flow on day 7 (Fig. 4). The patient was discharged on day 12. CT revealed an augmented intrahepatic portal vein on day 40 (Fig. 5). CT volumetry showed mildly increased liver volume on day 6 (1011.8 cm3) and day 40 (1011.4 cm3) in comparison to that before surgery (1004.6 cm3). An examination during a regular checkup found improved $NH_3$ (26 μg/dl), bilirubin (2.1 mg/dl), and PT-INR (1.19), representing liver function during a 3-month post-operative examination. The patient was able to discontinue lactulose and dietary supplementation with branched-chain amino acids 6 weeks after surgery.

## Discussion

The ductus venosus is a fetal vascular structure that connects the umbilical vein to the inferior vena cava, performing a crucial function within the fetal circulation because it bypasses the liver and directly provides oxygenated umbilical vein blood to the central circulation system [3]. Postnatal closure of the ductus venosus begins during the first minute after birth, and the vessel is functionally closed by day 18 [4]. The ductus venosus fails to close in very rare cases and persists as a left-sided extrahepatic portosystemic shunt. Congenital extrahepatic portosystemic shunts can be classified into two types by the pattern of anastomoses between the portal vein and IVC; type 1 has an end-to-side pattern, and type 2 has a side-to-side pattern [5]. PDV is categorized as type 2, in which intrahepatic portal venous supply is preserved.

Patent ductus venosus is extremely rare in adults. Fewer than 20 cases of PDV in adults have been reported in the literature [6–8]. Most adult cases are diagnosed with encephalopathy [7, 8], while children with PDV are psychiatrically asymptomatic in many cases and are diagnosed with hypergalactosemia, or sometimes cardiopulmonary disorder including congenital heart disease [2, 9, 10]. Kamimatsuse et al. reported eight cases of PDV in children, seven of which had no clinical symptoms. Although there is no explanation as to why some patients grow up without encephalopathy, the reduced tolerance to ammonia of the aging brain may be contributory [11].

The current patient experienced repeated encephalopathy, which became refractory to conservative therapy. Although a case with mild symptoms of portosystemic encephalopathy may be conservatively treated, shunt division by surgical banding or transcatheter intervention should be selected when the symptoms are not conservatively controlled, as in the present case. Retrograde transcatheter portography was performed to evaluate the intrahepatic portal flow and the possibility of shunt disconnection. PDV is associated with hypoplasty of the intrahepatic portal vein and shunt occlusion may cause severe complications, such as mesenteric venous congestion and bowel ischemia after shunt obstruction [10]. PVP increased immediately after occlusion in the current case, but returned to the normal range 1 hour after occlusion. This indicated that a fatal PVP elevation could thus be avoided after disconnection.

Treatment for PDV is still controversial. Transcatheter radiological occlusion using a steel coil has been reported, with the advantage of being less invasive [6, 7]. Although successful surgical ligation has been reported in some pediatric patients [1, 9, 15], interventional treatment has been selected in most adult cases to avoid life-threatening complications due to steep portal congestion [1, 12]. Although one group reported the application of this

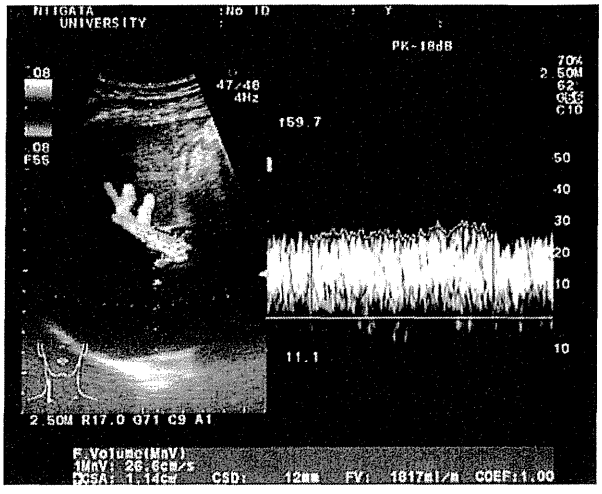


**Fig. 4** Post-operative echogram indicating markedly increased blood flow on day 7

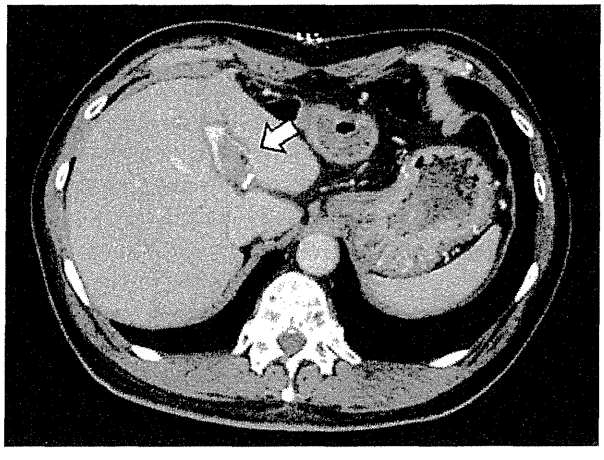

**Fig. 5** CT on day 6 revealed a portal thrombus in the umbilical portion close to the PDV stump (*white arrow*)

procedure to a case of large-diameter PDV in an adult [8], interventional embolization had a risk of migration in the present case. The results of the retrograde portography and the balloon occlusion test suggested that the shunt could be safely dissected in the current case and surgical treatment was selected, with the consent of the patient. A laparoscopic approach to a congenital portosystemic shunt has been reported by two groups, with positive results after surgery [13, 14]. The current case is the first report of laparoscopic surgery for PDV. The ductus venosus is an extrahepatic structure in itself and is not so difficult to band surgically, as discussed in other reports [1, 15]. There were no collateral vessels around the PDV and the vessel was easily isolated from the liver parenchyma.

We previously describe a case of a surgically resected portosystemic shunt that exhibited remarkable liver-volume augmentation 1 month after surgery [16]. In contrast, the present case of PDV exhibited only a mild increment in the liver volume. Most adult or older child patients have macroscopic liver atrophy or fibrosis [8–10]. Although a preoperative liver biopsy also revealed mild fibrosis in this case, the liver was not as atrophic as in the previous case, which may explain the difference in regrowth observed after shunt disconnection.

Despite preventive anti-coagulant therapy, the current patient developed portal thrombosis after surgery. Kamimatsuse et al. [9] also reported portal thrombosis occurring after surgical ligation of PDV. Portal thrombosis could arise in the stump of the splenic vein after splenectomy in cirrhotic patients due to stasis of venous flow in the stump of the splenic vein [17]. This may have caused thrombosis after dissection of the PDV. The site of dissection should be as close to the left portal branch as possible, and postoperative anti-coagulant therapy as well as evaluation with enhanced CT should be performed after either surgical division or banding for PDV.

In summary, this report presented an adult case of PDV that was successfully divided by laparoscopic surgery. Although a detailed and careful interventional evaluation for portal flow using a balloon occlusion test is absolutely imperative prior to surgery, a minimally invasive laparoscopic approach can be safely used for treating PDV.

**Conflict of interest** Y. Hara and the other co-authors have no conflict of interest to declare.

## References

1. Ikeda S, Yamaguchi Y, Sera Y, Ohshiro H, Uchino S, Ogawa M. Surgical correction of patent ductus venosus in three brothers. Dig Dis Sci. 1999;44:582–9.
2. Cho YK, Chang NK, Ma JS. Successful transcatheter closure of a large patent ductus venosus with the Amplatzer vascular plug II. Pediatr Cardiol. 2009;30:540–2.
3. Merkle EM, Gilkeson RC. Remnants of fetal circulation: appearance on MDCT in adults. Am J Roentgenol. 2005;185(2):541–9.
4. Fugelseth D, Lindemann R, Liestol K, Kiserud T, Langslet A. Ultrasonographic study of ductus venosus in healthy neonates. Arch Dis Child Fetal Neonatal Ed. 1997;77(2):F131–4.
5. Stringer MD. The clinical anatomy of congenital portosystemic venous shunts. Clin Anat. 2008;21(2):147–57.
6. Araki T, Kamada M, Okamoto Y, Arai S, Oba O. Coil embolization of a patent ductus venosus in a 52-day-old girl with congenital heart disease. Ann Thorac Surg. 2003;75:273–5.
7. Araki T, Konishi T, Yasuda S, Osada T, Araki T. Embolization of the patent ductus venosus in an adult patient. AJR Am J Roentgenol. 2003;180:716–8.
8. Shen B, Younossi ZM, Dolmatch B, Newman JS, Henderson JM, Ong JP, et al. Patent ductus venosus in an adult presenting as

pulmonary hypertension, right-sided heart failure, and portosystemic encephalopathy. Am J Med. 2001;110:657–60.
9. Kamimatsuse A, Onitake Y, Kamei N, Tajima G, Sakura N, Sueda T, et al. Surgical intervention for patent ductus venosus. Pediatr Surg Int. 2010;26:1025–30.
10. Yoshimoto Y, Shimizu R, Saeki T, Harada T, Sugio Y, Nomura S, et al. Patent ductus venosus in children: a case report and review of the literature. J Pediatr Surg. 2004;39:E1–5.
11. Raskin NH, Price JB, Fishman RA. Portal-systemic encephalopathy due to congenital intrahepatic shunts. N Engl J Med. 1964;270:225–9.
12. Barsky MF, Rankin RN, Wall WJ, Ghent CN, Garcia B. Patent ductus venosus: problems in assessment and management. Can J Surg. 1989;32(4):271–5.
13. Kimura T, Soh H, Hasegawa T, Sasaki T, Kuroda S, Yuri E, et al. Laparoscopic correction of congenital portosystemic shunt in children. Surg Laparosc Endosc Percutan Tech. 2004;14:285–8.
14. Nii A, Takehara HO, Kuyama H, Shimada M. Successful preemptive surgical division of type 2-congenital extrahepatic portosystemic shunt in children. J Med Invest. 2009;56:49–54.
15. Yagi H, Takada Y, Fujimoto Y, Ogura Y, Kozaki K, Ueda M, et al. Successful surgical ligation under intraoperative portal vein pressure monitoring of a large portosystemic shunt presenting as an intrapulmonary shunt: report of a case. Surg Today. 2004;34:1049–52.
16. Sato Y, Mitsuma C, Iwaya A, Kurosaki I, Shirai Y, Hatakeyama K. Resection of spleno-renal shunt resulting in enhanced liver volume in a patient with congenital portosystemic shunt concomitant with early gastric cancer. Review of Japanese cases. Dig Surg. 2001;18:74–8.
17. Kinjo N, Kawanaka H, Akahoshi T, Tomikawa M, Yamashita N, Konishi K, et al. Risk factors for portal venous thrombosis after splenectomy in patients with cirrhosis and portal hypertension. Br J Surg. 2010;97:910–6.

Hindawi Publishing Corporation
International Journal of Hepatology
Volume 2012, Article ID 410781, 6 pages
doi:10.1155/2012/410781

*Review Article*

# Hepatic Angiomyolipoma: Diagnostic Findings and Management

**Kenya Kamimura, Minoru Nomoto, and Yutaka Aoyagi**

*Division of Gastroenterology and Hepatology, Graduate School of Medical and Dental Sciences, Niigata University, Asahimachi 1-757, Chuo-ku, Niigata 951-8122, Japan*

Correspondence should be addressed to Kenya Kamimura, kenya-k@med.niigata-u.ac.jp

Received 22 October 2012; Accepted 2 December 2012

Academic Editor: Hiroshi Nishihara



Angiomyolipoma (AML) is a benign mesenchymal tumor that is frequently found in the kidney and, rarely, in the liver. The natural history of hepatic AML has not been clarified, and, because of the similar patterns in imaging studies, such as ultrasonography, computed tomography, and magnetic resonance imaging, some of these tumors have been overdiagnosed as hepatocellular carcinoma in the past. With an increase in the number of case reports showing detailed imaging studies and immunohistochemical staining of the tumor with human melanoma black-45, the diagnostic accuracy is also increasing. In this paper, we focused on the role of noninvasive imaging studies and histological diagnosis showing distinctive characteristics of this tumor. In addition, because several reports have described tumor progression in terms of size, recurrence after surgical resection, metastasis to other organs, and portal thrombosis, we summarized these cases for the management and discussed the indications for the surgical treatment of this tumor.

## 1. Introduction

Hepatic angiomyolipoma (HAML) is a rare benign mesenchymal liver tumor first described by Ishak [1] in 1976; it belongs to a group of perivascular epithelioid cell tumors called PEComa [2]. Until date, approximately 300 cases have been reported [3–10]; however, its natural history has not been clarified. The tumor composed of blood vessels, smooth muscle, and adipose cells and due to the variety of predominance of these tissues, its patterns in imaging studies have resulted in a difficulty in diagnosis and misdiagnosis of the tumor as hepatocellular carcinoma (HCC) in some cases [6, 11]. Therefore, the preoperative correct diagnosis has been difficult; however, recent advances in imaging diagnosis through a combination of ultrasonography (US), computed tomography (CT), magnetic resonance imaging (MRI), and angiography and specific immunohistochemical analysis of this tumor using human melanoma black-45 antigen (HMB-45) staining have resulted in accurate diagnosis and it is reported that the current accurate preoperative diagnosis was made in 25%–52% of cases [8, 9]. The majority of these tumors are believed to be clinically benign during a mean follow-up period of 6.8 years [11]; however, an increasing number of cases and aggressive changes including growth in size, recurrence after surgical resection, metastasis, and invasive growth pattern into the parenchyma and along the vessels have been reported. In this paper, we have focused on the characteristic features of this tumor shown in imaging studies and by histological analysis, summarized these cases showing aggressive patterns, and discussed management of the patients and indications for surgical treatment.

## 2. Natural History and Laboratory Findings

The natural history of this tumor has not been clarified. Most cases were found as incidental liver tumors upon health screening or imaging examinations for other diseases. It usually follows a benign clinical course while some patients visited hospitals with unspecific symptoms of abdominal discomfort, fullness, and other such complaints. More than half of the renal AML are considered to be associated with tuberous sclerosis which features the loss of heterozygosity at *TSC1* (9q34) and *TSC2* (16p13), while it is estimated to be 5–15% in the liver [6]. Thus the etiology of most of these tumors in the liver is unknown; most cases have no history of liver diseases or specific symptoms, and no changes in laboratory data are seen. Moreover, serum levels of the tumor markers alpha-fetoprotein, protein induced

by vitamin K absence or antagonist II, carcinoembryonic antigen, and carbohydrate antigen 19-9 were normal.

## 3. Imaging Studies

Since this tumor is composed of various tissues, such as lipomatous, myomatous, and angiomatous tissue in various proportions, the imaging studies show a wide array of features depending on the predominance of each tissue. The tumor showing the predominance of lipomatous tissue is likely to be correctly diagnosed; however, myomatous and angiomatous variant poses diagnostic problems since it is difficult to be distinguished from malignant tumors.

*3.1. Ultrasonography (US).* US images may vary depending on the tissue components affected by the tumor. High echogenic lesions can be observed because of lipomatous and myomatous tissue, and angiomatous tissue may result in low echoic lesions in tumor images (Figure 1(a)). If the tumor has predominance of lipomatous tissue, the differential diagnosis with hepatic hemangioma is difficult by sonography alone. Color doppler sonography shows punctiform or filiform vascular distribution pattern if the tumor has predominance of angiomatous tissue. Recent reports showed the diagnostic effectiveness of contrast-enhanced US (CEUS) [10, 13]. Li et al. reported that CEUS revealed the typical imaging characteristics of HAML, that is, an inhomogeneous hyperenhancing pattern in the arterial phase and prolonged enhancement during the portal and Kupffer phases.

*3.2. Computed Tomography (CT).* Plain CT showed homogeneous or heterogeneous low-density lesions, and contrast-enhanced dynamic CT showed highly enhanced lesions in the arterial phase, prolonged enhancement in the portal phase, and, occasionally, defective lesions in the late venous phase depending on the component of the tumor tissue. A density of less than 20 hounsfield units in plain CT is useful to determine the involvement of lipomatous tissue [14]. The difficulty is, however, to diagnose the tumor that is myomatous tissue and angiomatous variant. For this point, modification of size of region of interest in CT was reported to be effective for accurately diagnose renal angiomyolipoma from renal cell carcinoma [15].

*3.3. Angiography.* Abdominal angiography showed marked tumor staining in the arterial phase, which remained in the portal phase (Figure 1(b)). In some tumors, drainage of the hepatic veins can be observed in the late vascular phase. The first phase of CT during hepatic arteriography showed significant hypervascular lesions in the tumor (Figure 1(c)), and the second phase showed the remains of staining and defective lesions in other areas (Figure 1(d)). CT during arterial portography showed areas of defective tumors (Figure 1(d)) [12].

*3.4. Magnetic Resonance Imaging (MRI).* MRI is considered to be the best modality to determine the components of the tumor. Hyperintensity on the T2-weighted image and hyper- or hypointensity on the T1-weighted image are observed depending on the component of tumor tissue [8–10]. Lipomatous lesions may be determined as hyperintensity on the T1-weighted image; they may also be determined by the chemical shift imaging technique. Contrast-enhanced dynamic MRI using gadolinium or the hepatocyte-specific contrast agent gadolinium-ethoxybenzyl-diethylenetriamine pentaacetic acid showed early enhancement in the arterial phase followed by the prolonged enhancement in the portal phase and defective lesions in the hepatobiliary phase.

## 4. Pathological Findings

Macroscopic and magnifying glass view of the tumor showed a soft, white to yellow, and well-circumscribed tumor and range in size from 0.1 cm to greater than 36 cm [11]. No signs of chronic inflammation or fibrosis were seen in the surrounding liver tissue. Because HAML comprises lipomatous, myomatous, and angiomatous tissues, microscopic examination showed a mixture of blood vessels, specialized smooth muscle cells, and adipose cells with atypical changes in classic HAML (Figures 2(a) and 2(b)). This variation of mixture levels in one tumor reflected the differences in imaging studies and made accurate diagnosis difficult. It is believed that majority of the HAMLs behave in a benign fashion and even if some cases showed invasive growth pattern into the adjacent hepatic parenchyma, portal triad (Figure 2(c)), and hepatic vein [11]. Tumor cells, especially myomatous cells, were stained positive for HMB-45 in most tumors (Figure 2(d)), for CD34 in the endothelial cells of the blood vessels and for smooth muscle actin in spindle smooth muscle cells. HMB-45 is an antibody that reacts with an oncofetal premelanosome-associated glycoprotein 2, found in neoplastic melanocytes. Also CD63, CD67, desmin, S100, and EMA may also be positive but not specific. These cells were negative for cytokeratin 18, cytokeratin 19, CAM 5.2, hepatocyte paraffin-1. Therefore, the identification of lipomatous, myomatous, and angiomatous tissue by a positive reaction to HMB-45 currently provides the only evidence of HAML [4–6, 18] and can be useful for defining from the other liver tumors such as HCC after the tumor biopsy and surgical resection followed by these immunohistochemical stainings. Although favorable prognosis can be expected for this tumor since the majority of the tumors are benign, however recently, the number of reports of HAML showing malignant potential has increased [3, 5, 8, 9, 12, 16–24] which revealed significant growth, recurrence, metastasis, and poor prognosis summarized in Table 1. Among those cases, Deng et al. reported in their case that HAML showed atypical angiomatous, epithelioid components with pleomorphic and frequent mitosis in the center of the large tumor displayed p53 immunoreactivity, and mutation at exon 7 for p53 and resulted in vascular invasion, distant metastasis, and fatal outcomes [23]. These results indicate that the HMB-45 staining, mitotic analysis by MIB-1 (Ki67), and p53 reactivity following the fine-needle biopsy of the tumor might be useful for the diagnosis of the tumor and its malignant potential.

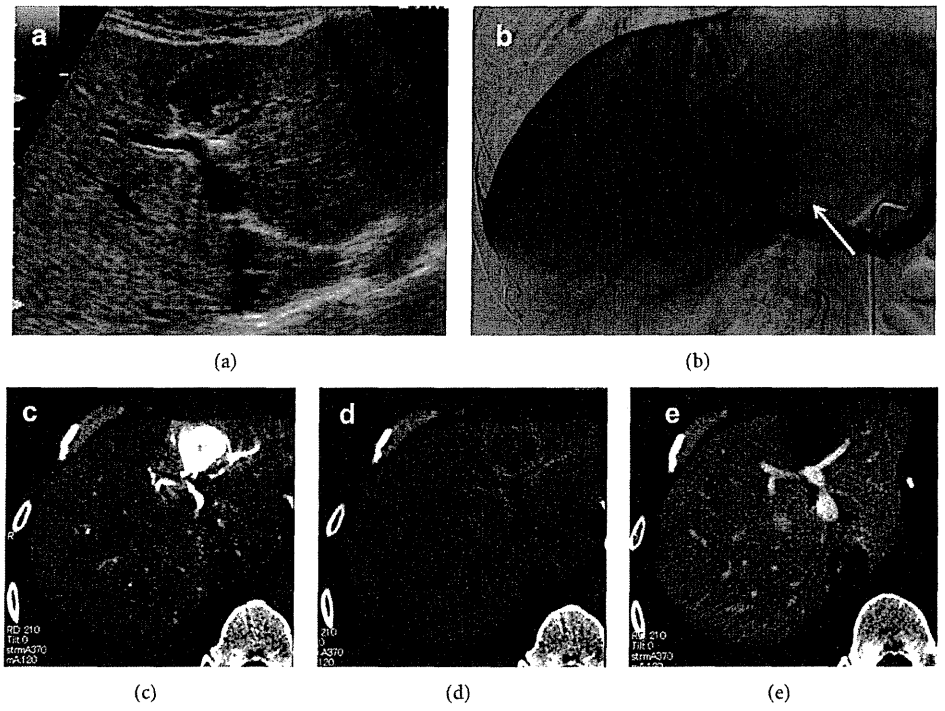


FIGURE 1: Imaging studies of HAML: (a) ultrasonography and (b) angiography. White arrow indicates the tumor staining in the portal venous phase. (c) 1st phase of CTA, (d) 2nd phase of CTA, and (e) CTAP. ((e) is from [12] with permission from Springer).

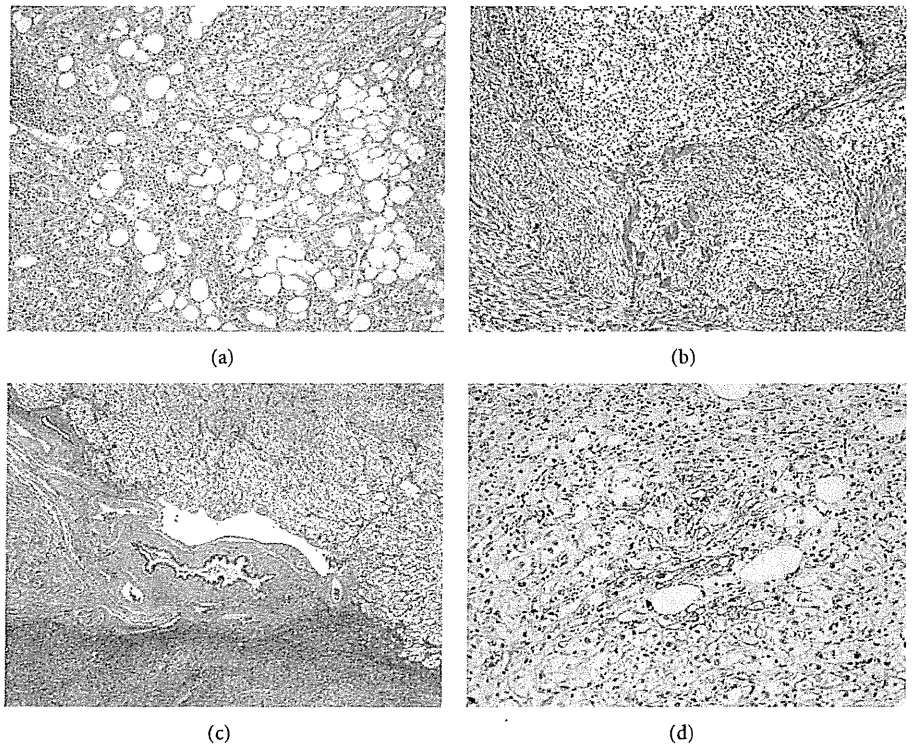


FIGURE 2: Pathological findings of HAML. The tumor was consisted of lipomatous, myomatous, and angiomatous tissue with variance. (a) A part of the tumor showed predominance of lipomatous tissue and the center of the tumor showed predominance of myomatous and angiomatous tissue (b). (c) The tumor showed aggressive growth pattern infiltrating into the portal vein (HE staining, ×40). (d) Tumor cells were positive for HMB-45 staining (×100) ((a) is from [12] with permission from Springer).

Table 1: Summary of hepatic angiomyolipoma with progressive growth, recurrence, and metastasis.

| Case | Author | Tumor size (cm) | Tumor growth | Resection | Invasive growth | Portal vein thrombus | Recurrence | Metastasis | Prognosis | Clinical features |
|---|---|---|---|---|---|---|---|---|---|---|
| 1 | Ohmori et al. [16] | Tumor grew to 18 cm | + | − | + | N/A | − | − | D | Liver dysfunction |
| 2 | Dalle et al. [17] | Tumor grew from 15 to 26 cm in 5 years | + | + | + | + | +, 15 cm | +, peritoneum, liver | D | |
| 3 | Flemming et al. [18] | 0.5 and 10 cm | + | + | + | − | +, 20 cm | +, liver | A | Second resection was performed |
| 4 | Kamimura et al. [12] | 3.5 | + | + | + | + | − | − | A | |
| 5 | Rimola et al. [19] | Tumor grew from 6 to 11 in 8 years | + | − | − | N/A | N/A | N/A | A | |
| 6 | Chang et al. [9] | Tumor grew from 8 to 27 in a year | + | + | − | − | N/A | − | A | |
| 7 | Croquet et al. [20] | 19 | + | + | N/A | N/A | +, 33 cm | − | A | Second resection was performed |
| 8 | Rouquie et al. [21] | 9 | N/A | + | + | + | − | − | A | |
| 9 | Nguyen et al. [22] | 11 | N/A | + | + | + | + | +, liver, peritoneum, gastrohepatic omentum, and retroperitoneum. | D | |
| 10 | Deng et al. [23] | 18 | N/A | + | + | + | +, 11 cm | +, lung | D | |
| 11 | Yang et al. [3] | 13 | N/A | + | + | + | + | +, liver, lung | D | |
| 12 | Parfitt et al. [24] | 14 | N/A | + | + | N/A* | + | +, trapezius muscle, lung, pancreas | D | |
| 13 | Ding et al. [8] | 8 | N/A | + | N/A | N/A | + | − | D | |

N/A: information was not applicable.
D: dead and A: alive.
*Portal vein invasion was found in recurrent tumors.

## 5. Patient Management

Since HAML usually follows benign clinical courses, the majority of the cases can be conservatively treated. However, as not a few cases showed aggressive pattern in their courses [3, 5, 8, 9, 12, 16–24] and because of the low level of accurate diagnoses by imaging studies, and because of the possibility of dissemination of tumor cells into the peritoneal cavity if a tumor is malignant, tumor biopsy has been avoided, and many HAMLs have been surgically resected [3, 8, 9]. With the increasing number of resected samples, careful comparisons of imaging studies and pathological findings have been performed [8, 9, 12, 23]. Therefore, once HAML has been diagnosed by imaging studies, a fine-needle biopsy should be performed to make an accurate diagnosis [19] and to confirm the predominance of the tissue components, the existence of pleomorphic nuclei with high proliferation activity, p53 immunoreactivity, and mutation in p53 if possible. If the aggressive patterns such as vascular invasion, high proliferation of the tumor cells, p53 immunoreactivity were marked [23], or when the imaging findings and biopsy cannot provide a definitive diagnosis, or if the patients have abdominal symptoms, surgical resection should be considered.

## 6. Discussion

HAML is considered to be a benign mesenchymal tumor [1], and nonsurgical treatment with conservative management involving close followup is therefore suggested for patients with asymptomatic tumors smaller than 5 cm, which have been proved to be a typical HAML by fine-needle aspiration biopsy [3]. As a fact the renal angiomyolipoma often showed perirenal invasion, involvement of the renal vein, and the inferior vena cava, that are not considered as signs of malignant behavior and the angiomatous, epithelioid monophasic or pleomorphic variant might be associated with the aggressive behavior and cellular atypia, mitotic activity, and metastatic lesions are the criteria for the malignant renal angiomyolipoma. However, due to the difficulties in diagnosis by imaging studies, many HAMLs have been surgically resected and have been followed closely for a long period. In addition, by careful analysis of these recent cases [3, 5, 8, 9, 12, 16–24] summarized in Table 1, it was revealed that, although rare, HAMLs may have malignant potential, which may be distinguished by aggressive patterns characterized by (1) significant changes in size in short period; (2) a change of tumor composition (Cases 1, 2, 5, and 6) [9, 16, 17, 19]; (3) metastases to the other organs (Cases 1, 9, and 10) [17, 22, 23]; (4) recurrence after curative surgical resection (Cases 3, 7, 9, 10, 11, 12, and 13) [3, 8, 18, 20, 22–24]; and (5) invasive growth into the vessels (Cases 2, 4, 8, 9, and 10) [12, 17, 21–23].

Ohmori et al. reported the first possibly malignant case [16], which showed that a significant increase in the tumor size resulted in liver dysfunction. Fatal progression was observed in nine cases listed by multiple recurrences [3, 8, 18, 20, 22–24] and metastases to the liver, peritoneum, retroperitoneal region, gastrohepatic omentum, pancreas, and lung [17, 22, 23]. The cases reported by Chang [9], Rouquie [21], and us [12] underwent surgical resection, with a suspicious of aggressive patterns and no recurrence has occurred. We also reported that portal thrombosis, that is, high-grade portal vein invasion, found in five cases in Table 1 (Cases 2, 8, 9, 10, and 11) [3, 17, 21–23] may be a clinical marker of the malignant potential and transformation of HAML [12] as it resulted in a significantly aggressive disease and fatal course in 4 cases with multiple recurrences and metastases. This finding might be able to be detected by imaging studies as similar to HCC. In addition, pathological findings of atypical epithelioid component with high proliferation activity, p53 immunoreactivity, and mutation in p53 might be predictive markers for malignant transformation [23]. Based on these reports, as recommended by previous papers [3, 8, 9], long-term follow-up of HAML is necessary after its diagnosis by imaging studies and biopsy specimens and curative surgical treatment. The majority of HAMLs behave as a benign tumors and conservative follow-up may be recommended [25]; however, with increasing number of the reports showing potentially malignant behavior, prompt surgical resection is essential for better prognosis of this tumor.

## 7. Conclusion

We have reviewed noninvasive imaging studies and the role of histological diagnosis showing distinctive characteristics of HAML to increase the rate of accurate diagnoses. In addition, we summarized the cases that showed progressive patterns of the tumor and concluded that a careful followup of the tumor even after the final diagnosis is necessary. We propose that tumor resection is indicated in the following scenarios: (1) the patients show symptoms; (2) the tumor shows an aggressive growth; (3) the tumor shows invasive growth into the vessels evidenced by fine-needle biopsy or imaging studies; (4) the component of the tumor shows atypical epithelioid pattern, high proliferation activity, and/or p53 immunoreactivity; and (5) a definitive diagnosis cannot be made by imaging and pathological studies from malignant tumors.

## Conflict of Interests

The authors declare that they have no current financial arrangement or affiliation with any organization that may have a direct influence on their work.

## Acknowledgment

The authors acknowledge Takao Tsuchida, Division of Gastroenterology and Hepatology, Niigata University, for his excellent assistance for histological stainings.

## References

[1] K. G. Ishak, "Mesenchymal tumors of the liver," in *Hepatocellular Carcinoma*, pp. 247–307, John Wiley & Sons, New York, NY, USA, 1976.

[2] F. Bonetti, M. Pea, G. Martignoni et al., "PEC and sugar," *The American Journal of Surgical Pathology*, vol. 16, no. 3, pp. 307–308, 1992.

[3] C. Y. Yang, M. C. Ho, Y. M. Jeng et al., "Management of hepatic angiomyolipoma," *Journal of Gastrointestinal Surgery*, vol. 11, no. 4, pp. 452–457, 2007.

[4] A. Nonomura, Y. Mizukami, N. Takayanagi et al., "Immunohistochemical study of hepatic angiomyolipoma," *Pathology International*, vol. 46, no. 1, pp. 24–32, 1996.

[5] N. Ren, L. X. Qin, Z. Y. Tang, Z. Q. Wu, and J. Fan, "Diagnosis and treatment of hepatic angiomyolipoma in 26 cases," *World Journal of Gastroenterology*, vol. 9, no. 8, pp. 1856–1858, 2003.

[6] W. M. S. Tsui, R. Colombari, B. C. Portmann et al., "Hepatic angiomyolipoma: a clinicopathologic study of 30 cases and delineation of unusual morphologic variants," *The American Journal of Surgical Pathology*, vol. 23, no. 1, pp. 34–48, 1999.

[7] L. Xie, J. Jessurun, J. C. Manivel, and S. E. Pambuccian, "Hepatic epithelioid angiomyolipoma with trabecular growth pattern: a mimic of hepatocellular carcinoma on fine needle aspiration cytology," *Diagnostic Cytopathology*, vol. 40, no. 7, pp. 639–650, 2012.

[8] G. H. Ding, Y. Liu, M. C. Wu et al., "Diagnosis and treatment of hepatic angiomyolipoma," *Journal of Surgical Oncology*, vol. 103, no. 8, pp. 807–812, 2011.

[9] Z. G. Chang, J. M. Zhang, J. Q. Ying, and Y. P. Ge, "Characteristics and treatment strategy of hepatic angiomyolipoma: a series of 94 patients collected from four institutions," *Journal of Gastrointestinal and Liver Diseases*, vol. 20, no. 1, pp. 65–69, 2011.

[10] S. Krebs, I. Esposito, C. Lersch et al., "Preoperative radiological characterization of hepatic angiomyolipoma using magnetic resonance imaging and contrast-enhanced ultrasonography: a case report," *Journal of Medical Case Reports*, vol. 26, no. 5, article 481, 2011.

[11] A. Nonomura, Y. Enomoto, M. Takeda et al., "Invasive growth of hepatic angiomyolipoma; a hitherto unreported ominous histological feature," *Histopathology*, vol. 48, no. 7, pp. 831–835, 2006.

[12] K. Kamimura, A. Oosaki, S. Sugahara et al., "Malignant potential of hepatic angiomyolipoma: case report and literature review," *Clinical Journal of Gastroenterology*, vol. 3, no. 2, pp. 104–110, 2010.

[13] R. Li, X. Zhang, X. Hua et al., "Real-time contrast-enhanced ultrasonography of resected and immunohistochemically proven hepatic angiomyolipomas," *Abdominal Imaging*, vol. 35, no. 6, pp. 676–682, 2010.

[14] A. Nonomura, Y. Mizukami, and M. Kadoya, "Angiomyolipoma of the liver: a collective review," *Journal of Gastroenterology*, vol. 29, no. 1, pp. 95–105, 1994.

[15] M. S. Davenport, A. M. Neville, J. H. Ellis, R. H. Cohan, H. S. Chaudhry, and R. A. Leder, "Diagnosis of renal angiomyolipoma with hounsfield unit thresholds: effect of size of region of interest and nephrographic phase imaging," *Radiology*, vol. 260, no. 1, pp. 158–165, 2011.

[16] T. Ohmori, N. Arita, N. Uraga et al., "Giant hepatic angiomyolipoma," *Histopathology*, vol. 15, no. 5, pp. 540–543, 1989.

[17] I. Dalle, R. Sciot, R. de Vos et al., "Malignant angiomyolipoma of the liver: a hitherto unreported variant," *Histopathology*, vol. 36, no. 5, pp. 443–450, 2000.

[18] P. Flemming, U. Lehmann, T. Becker, J. Klempnauer, and H. Kreipe, "Common and epithelioid variants of hepatic angiomyolipoma exhibit clonal growth and share a distinctive immunophenotype," *Hepatology*, vol. 32, no. 2, pp. 213–217, 2000.

[19] J. Rimola, J. Martín, J. Puig, A. Darnell, and D. Gil, "Hepatic angiomyolipoma: progressive changes in size and tumor composition," *Abdominal Imaging*, vol. 28, no. 5, pp. 665–667, 2003.

[20] V. Croquet, C. Pilette, C. Aube et al., "Late recurrence of a hepatic angiomyolipoma," *European Journal of Gastroenterology and Hepatology*, vol. 12, no. 5, pp. 579–582, 2000.

[21] D. Rouquie, P. Eggenspieler, J. P. Algayres, D. Béchade, P. Camparo, and B. Baranger, "Malignant-like angiomyolipoma of the liver: report of one case and review of the literature," *Annales de Chirurgie*, vol. 131, no. 5, pp. 338–341, 2006.

[22] T. T. Nguyen, B. Gorman, D. Shields et al., "Malignant hepatic angiomyolipoma: report of a case and review of literature," *The American Journal of Surgical Pathology*, vol. 32, no. 5, pp. 793–798, 2008.

[23] Y. F. Deng, Q. Lin, and S. H. Zhang, "Malignant angiomyolipoma in the liver: a case report with pathological and molecular analysis," *Pathology, Research and Practice*, vol. 204, no. 12, pp. 911–1018, 2008.

[24] J. R. Parfitt, A. J. Bella, J. I. Izawa, and B. M. Wehrli, "Malignant neoplasm of perivascular epithelioid cells of the liver: late widespread metastases with long-term follow-up," *Archives of Pathology and Laboratory Medicine*, vol. 130, no. 8, pp. 1219–1222, 2006.

[25] A. A. Petrolla and W. Xin, "Hepatic angiomyolipoma," *Archives of Pathology and Laboratory Medicine*, vol. 132, no. 10, pp. 1679–1682, 2008.

Kamimura et al. BMC Gastroenterology 2012, 12:127
http://www.biomedcentral.com/1471-230X/12/127

BMC Gastroenterology

RESEARCH ARTICLE Open Access

# Phase I study of miriplatin combined with transarterial chemotherapy using CDDP powder in patients with hepatocellular carcinoma

Kenya Kamimura, Takeshi Suda*, Yasushi Tamura, Masaaki Takamura, Takeshi Yokoo, Masato Igarashi, Hirokazu Kawai, Satoshi Yamagiwa, Minoru Nomoto and Yutaka Aoyagi

**Abstract**

**Background:** There is no standard therapeutic procedure for the hepatocellular carcinoma (HCC) in patients with poor hepatic reserve function. With the approval of newly developed chemotherapeutic agent of miriplatin, we have firstly conducted the phase I study of CDDP powder (DDP-H) and miriplatin combination therapy and reported its safety and efficacy for treating unresectable HCC in such cases. To determine the maximum tolerated dose (MTD) and dose-limiting toxicity (DLT) for the combination of transarterial oily chemoembolization (TOCE) and transarterial chemotherapy (TAC) using miriplatin and DDP-H for treating unresectable hepatocellular carcinoma (HCC).

**Methods:** Transarterial chemotherapy using DDP-H was performed through the proper hepatic artery targeting the HCC nodules by increasing the dose of DDP-H (35–65 mg/m$^2$) followed by targeting the HCC nodules by transarterial oily chemoembolization with miriplatin.

**Results:** A total of nine patients were enrolled in this study and no DLT was observed with any dose of DDP-H in all cases in whom 80 mg (median, 18–120) miriplatin was administered. An anti-tumour efficacy rating for partial response was obtained in one patient, while a total of four patients (among eight evaluated) showed stable disease response, leading to 62.5% of disease control rate. The pharmacokinetic results showed no further increase in plasma platinum concentration following miriplatin administration.

**Conclusion:** Our results suggest that a combination of DDP-H and miriplatin can be safely administered up to their respective MTD for treating HCC.

**Trial registration:** This study was registered with the University Hospital Medical Information Network Clinical Trials Registry (UMIN-CTR000003541).

**Keywords:** Miriplatin, Hepatocellular carcinoma, Cisplatin powder, Phase I clinical trial

## Background

Hepatocellular carcinoma (HCC) is the most common type of liver cancer [1] and various therapeutic options have been developed by focusing on the specific tumour stage and hepatic functional reserve [2-9]. A variety of transarterial treatments have been provided to cases at relatively advanced stages [3], and these treatments were roughly divided into the following three groups: transarterial chemoembolization (TACE), transarterial oily chemoembolization (TOCE) and transarterial chemotherapy (TAC), based on the likelihood of deteriorating hepatic reserve. TACE involves hepatic arterial injections of chemotherapeutic agents combined with embolizing materials. TOCE is solely an arterial administration of a combination of chemotherapeutic agents and oily contrast medium of lipiodol ultra fluid (Laboratory Guerbet, Aulnay-sous-Bois, France), while in TAC, chemotherapeutic agents alone are infused through the hepatic artery. Although TACE is only a transarterial procedure, for which therapeutic efficacy has been proved in randomised prospective controlled studies, the deterioration of hepatic reserve is estimated at 20%–58%, mainly because

* Correspondence: suda@med.niigata-u.ac.jp
Division of Gastroenterology and Hepatology, Graduate School of Medical and Dental Sciences, Niigata University, Niigata, Japan

of ischaemic damage to the nontumourous background liver [10,11], inferring a higher risk of unfavourable reduction in hepatic reserve function in cases with poor hepatic reserve. Therefore, to develop a safe and efficient transarterial therapeutic procedure in such cases, other effective means of performing TOCE, TAC, and TOCE + TAC have been tested [5,12-15].

TACE and TOCE were recently compared in a randomised phase III trial using zinostatin stimalamer dissolved in lipiodol [12] with subsequent arterial embolization (TACE) or without embolization (TOCE). Interestingly, the results showed no improvement in survival rates by performing embolization and TOCE represented to be a therapeutic option for HCC patients with low hepatic reserve. However, two major concerns with TOCE are: 1) the method of combining water-based chemotherapeutic agents with oily lipiodol in a stable formulation; and 2) that TOCE is unable to target wide area of the liver as it reduces the hepatic arterial flow, although tentative, that may result in hepatic failure. For first concern, Miriplatin, a third-generation platinum derivative with lipophilic moiety that forms a suspension with lipiodol, was recently developed and approved for clinical use in Japan as a novel chemotherapeutic agent for HCC [16-21] with promising results [22-24]. For second concern, as TAC requires no embolization, that can be injected in wide area and its anti-tumour effect has been reported in several studies [5,13-15], followed by the promising results from a multicentre phase II study in patients with unresectable HCC using cisplatin (CDDP), a first-generation platinum agent, in which the response rate was recorded as 33.8% [13], it might be effective to treat wide area of the liver with poor hepatic reserve function. In addition, the first-pass kinetics [25] of CDDP by TAC contribute to the anti-tumor effect and decrease the adverse systemic events [5]. Since highly concentrated CDDP powder for TAC (DDP-H, IA-call®; Nippon Kayaku Co., Ltd) is available in Japan, TAC is now widely used in Japan to treat multiple small tumours or patients with poor hepatic reserve [5,13,26].

Based on these results and the advances in the development of new chemotherapeutics, it is reasonable to consider the combination therapy of CDDP-TAC with miriplatin-TOCE to treat advanced stage HCC with poor hepatic reserve function safely and effectively. Therefore, in this study we conducted a phase I dose-escalation study on DDP-H-TAC followed by miriplatin-TOCE to determine the maximum tolerated dose (MTD) and dose-limiting toxicity (DLT) in unresectable HCC. The safety issue with regard to the combination of two platinum-based chemotherapeutic agents will be discussed by referencing the pharmacokinetics of platinum.

## Methods

### Patient selection

Patients with HCC were considered eligible for the study if they fulfilled the following criteria: 20–80 years of age; at least one measurable tumour blush on angiography; histologically and/or clinically diagnosed HCC; no other therapeutic treatment was found to be effective or appropriate to their condition, according to the Japanese guidelines for HCC treatment; an Eastern Cooperative Oncology performance status of 0–2; adequate hepatic function (Child–Pugh, score ≤7; total bilirubin, ≤3.0 mg/dl; albumin, ≥3.0 g/dl); adequate haematological function (neutrophils, ≥1,500/mm$^3$; platelets, ≥50,000/mm$^3$; haemoglobin, ≥8.0 g/dl); adequate renal function (creatinine clearance, ≥50 ml/min adjusted for 1.73 m$^2$ of body surface area); serum amylase, ≤324 IU/dl and an interval of 4 weeks or more since previous therapy.

All nodules were radiologically diagnosed as HCC when they satisfied at least one of the following criteria based on CT or MRI: typical haemodynamics of classical HCC (substantial enhancement during arterial phase followed by a washout with 'corona-like' peripheral enhancement in equilibrium phase) and similar characteristics of coexisting nodules that had been diagnosed as HCC. All eligible HCC cases were recurrent with a history of CDDP administration in eight patients. Patients with the following characteristics were considered ineligible: massive pleural effusion and/or ascites refractory to treatment; active cancer other than HCC; active infectious disease; active haemorrhagic state; severe mental disorder; hepatic encephalopathy; history of allergic reaction to iodine phase contrast and/or platinum agents; ongoing interferon therapy and difficulty with oral food intake. This study was approved by the institutional review board of Niigata University Hospital and was registered with the University Hospital Medical Information Network Clinical Trials Registry (UMIN-CTR 000003541). Written informed consent was obtained from all patients and the study protocol conformed to the ethical guidance of the 1975 Declaration of Helsinki.

### Method of administration

CDDP powder, DDP-H (Nippon Kayaku Co., Ltd. Tokyo, Japan), was solubilised in saline at a concentration of 100 mg/70 ml immediately before use and infused into the entire liver through the proper hepatic artery at a rate of 126 ml/h, providing in total 35 mg/m$^2$. This was followed by TOCE with miriplatin, prepared according to the instructions, through the nutrient vessels of the target tumour using a maximal dose showing corresponding drainage portal veins up to a volume of 6 ml. If no DLT was recorded, the same regimen was carried out by increasing DDP-H by 15 mg/m$^2$, based on the modified Fibonacci method in which DLT is defined as adverse

events of grade ≥3 in nonhaematological or grade ≥4 in haematological toxicity, according to the NCI-CTCAE version 4.0. If any of the three patients showed as having DLT, three more patients were enrolled. MTD was judged to have been exceeded when two patients showed DLT. MTD was defined as the maximum dose where no more than two of the six patients experienced DLT. If two or more cases were already suffering from DLT at the initial dose of 35 mg/m$^2$, this dose was reduced by 10 mg/m$^2$ to 15 mg/m$^2$.

### Evaluation of anti-tumour effects

Anti-tumour response was evaluated from CT images obtained before and 3 months after treatment. Evaluation was performed in accordance with the modified Response Evaluation Criteria in Solid Tumors (RECIST) guideline, a new response evaluation criteria in solid tumours [27]. The tumour markers of AFP and DCP were followed at appropriate time periods for each patient.

### Platinum pharmacokinetics

Total plasma platinum concentration was measured and pharmacokinetic evaluation performed for all patients. Plasma samples were collected in heparinised tubes at 24 h and 7 days following the administration of DDP-H and miriplatin. As reference, 50 mg/m$^2$ (80 mg/body) of CDDP in liquid form was administered through the proper hepatic artery for the entire liver at a rate of 1 mg/min, and the concentration was quantified before the administration and at 0.5, 1.0, 1.5, 2, 4, 12 and 24 h after administration. Plasma platinum concentration was measured by atomic absorption spectrometry (Nac Co., Ltd., Tokyo, Japan).

## Results

### Patient characteristics

A total of nine eligible patients were enrolled in this study from July to October 2010 and divided into three groups; none of the three patients from each group developed DLT at DDP-H dose levels of 35 (level 1), 50 (level 2) and 65 (level 3) mg/m$^2$. Patient characteristics

**Table 1 Patient characteristics**

| Group | Level 1 | | | Level 2 | | | Level 3 | | |
|---|---|---|---|---|---|---|---|---|---|
| CDDP (mg/m$^2$) | 35 | | | 50 | | | 65 | | |
| Case number | 1 | 2 | 3 | 4 | 5 | 6 | 7 | 8 | 9 |
| Age (years) | 80 | 62 | 80 | 78 | 61 | 80 | 63 | 79 | 80 |
| Gender (M, Male/F, Female) | M | M | M | M | M | M | M | F | F |
| Performance status | 1 | 0 | 0 | 0 | 0 | 0 | 0 | 0 | 0 |
| HBV infection | - | - | - | - | - | - | + | - | - |
| HCV infection | + | + | - | - | - | + | - | + | - |
| Alcohol | - | - | + | + | + | - | - | - | - |
| Autoimmune hepatitis | - | - | - | - | - | - | - | - | + |
| Child-Pugh Score | 6 | 6 | 5 | 6 | 6 | 7 | 5 | 6 | 6 |
| Recurrence (Y, Yes/N, No) | Y | Y | Y | Y | Y | Y | Y | Y | Y |
| Interval to previous therapy (M) | 6 | 8 | 6 | 23 | 10 | 21 | 13 | 19 | 3 |
| Previous therapy | TACE | TAC | TACE | TACE | TAC | TACE | TAC | TACE | TACE |
| History of CDDP Administration | Y | Y | N | Y | Y | Y | Y | Y | Y |
| Number of tumors | 3 | 2 | 1 | >5 | >5 | 4 | 4 | >5 | >5 |
| Maximum tumor size (mm) | 15 | 15 | 14 | 20 | 10 | 34 | 24 | 10 | 30 |
| Vascular invasion (Y, Yes/N, No) | N | N | N | N | N | N | N | N | N |
| Metastasis (Y, Yes/N, No) | N | N | N | N | N | N | N | N | N |
| Stage (UICC) | II | II | I | II | II | II | II | II | II |
| Tumor location (PAMLC) | PA | ML | ML | AM | ML | M | P | A | PA |
| BSA (m$^2$) | 1.486 | 1.6 | 1.457 | 1.5 | 1.72 | 1.68 | 1.415 | 1.538 | 1.538 |
| Ccr (ml/min) | 68 | 118 | 75 | 89 | 121 | 92 | 83 | 95 | 85 |
| CDDP (mg/body) | 52 | 56 | 51 | 75 | 86 | 84 | 92 | 100 | 100 |
| Miriplatin (mg/body) | 86 | 18 | 80 | 120 | 60 | 60 | 74 | 100 | 120 |

TACE, transarterial chemoembolization; TAC, transarterial chemotherapy. Tumour location: P, posterior segment; A, anterior segment; M, medial segment; L, lateral segment; C, caudal segment. BSA, body surface area; Ccr, creatinine clearance.

before treatment are summarised in Table 1. Performance status was 0 in eight patients and 1 in one patient (case 1). The aetiology of liver cirrhosis was HBV infection ($n$ = 1), HCV infection ($n$ = 4), alcoholic abuse ($n$ = 3) and autoimmune hepatitis ($n$ = 1). Residual liver function was relatively good with a median Child–Pugh score of 6, eight patients in grade A and one in grade B, and no marked renal dysfunction was observed. All patients had a history of HCC treatment; eight patients, other than case 3, had a history of DDP-H-TAC followed by epirubicin-TOCE.

The total dose of DDP-H administered was 51, 52 and 56 mg/body at level 1; 75, 84 and 86 mg/body at level 2 and 92, 100 and 100 mg/body at level 3. Total dose of miriplatin administered was 18, 80 and 86 mg at level 1; 60, 60 and 120 mg at level 2 and 74, 100 and 120 mg at level 3. All nine patients were assessed for toxicity of CDDP combined with miriplatin and for the pharmacokinetics of plasma platinum concentration. One patient underwent radio frequency ablation (RFA) before response evaluation, and thus eight patients were assessed for anti-tumour response.

### Toxicity

Haematological and nonhaematological toxicity in all patients was evaluated using NCI-CTCAE (National Cancer Institute Common Terminology Criteria for Adverse Events) version 4.0, summarised in Table 2. No grade ≥3 in nonhaematological or grade ≥4 in haematological toxicity was observed. One patient (case 4 in the level 2 group) developed grade 3 neutropenia (reduced from 3000/mm$^2$ to 1710/mm$^2$, 6 weeks after injection) and subsequently recovered over 2 weeks. All three groups showed a grade 2 increase in aspartate aminotransferase and alanine aminotransferase (cases 3, 5, 6 and 9) and grade 1–2 hypoalbuminaemia (cases 1, 2, 5, 7 and 9). No marked increase was noted in creatinine, except in case 7, which showed a transient increase of 1.13 times higher than baseline level 4 days after the administration of 65 mg/m$^2$ CDDP combined with 74 mg/body miriplatin. The most frequent adverse event was grade 1 monophasic fever, which was observed in cases 1, 4, 8 and 9 receiving 86, 120, 100 and 120 mg/body of miriplatin, respectively. Therefore, in this clinical study, the MTD of CDDP in combination with miriplatin was

**Table 2 Haematological and nonhaematological toxicity**

| | Level 1 | | | | Level 2 | | | | Level 3 | | | |
|---|---|---|---|---|---|---|---|---|---|---|---|---|
| | n = 3 | | | | n = 3 | | | | n = 3 | | | |
| | Grade | | | | | | | | | | | |
| Hematological toxicity (grade) | 1 | 2 | 3 | 4 | 1 | 2 | 3 | 4 | 1 | 2 | 3 | 4 |
| White blood cell decreased | 0 | 1 | 0 | 0 | 0 | 0 | 1 | 0 | 0 | 0 | 0 | 0 |
| Neutrophil count decreased | 0 | 1 | 0 | 0 | 0 | 0 | 1 | 0 | 0 | 0 | 0 | 0 |
| Platelet count decreased | 0 | 1 | 0 | 0 | 0 | 0 | 0 | 0 | 2 | 0 | 0 | 0 |
| Anemia | 0 | 1 | 0 | 0 | 0 | 0 | 0 | 0 | 0 | 0 | 0 | 0 |
| Nonhematological toxicity (grade) | 1 | 2 | 3 | 4 | 1 | 2 | 3 | 4 | 1 | 2 | 3 | 4 |
| AST increased | 0 | 1 | 0 | 0 | 1 | 1 | 0 | 0 | 0 | 1 | 0 | 0 |
| ALT increased | 0 | 1 | 0 | 0 | 1 | 1 | 0 | 0 | 0 | 1 | 0 | 0 |
| Blood bilirubin increased | 0 | 0 | 0 | 0 | 1 | 0 | 0 | 0 | 1 | 0 | 0 | 0 |
| INR increased | 0 | 0 | 0 | 0 | 0 | 0 | 0 | 0 | 0 | 0 | 0 | 0 |
| Hypoalbuminemia | 0 | 2 | 0 | 0 | 0 | 1 | 0 | 0 | 1 | 0 | 0 | 0 |
| Creatinine increased | 0 | 0 | 0 | 0 | 0 | 0 | 0 | 0 | 1 | 0 | 0 | 0 |
| Anorexia | 0 | 0 | 0 | 0 | 0 | 0 | 0 | 0 | 1 | 0 | 0 | 0 |
| Nausea | 0 | 0 | 0 | 0 | 0 | 0 | 0 | 0 | 0 | 0 | 0 | 0 |
| Vomiting | 0 | 0 | 0 | 0 | 0 | 0 | 0 | 0 | 0 | 0 | 0 | 0 |
| Fever | 1 | 0 | 0 | 0 | 1 | 0 | 0 | 0 | 2 | 0 | 0 | 0 |
| Diarrhea | 0 | 0 | 0 | 0 | 0 | 0 | 0 | 0 | 0 | 0 | 0 | 0 |
| Fatigue | 0 | 0 | 0 | 0 | 0 | 0 | 0 | 0 | 1 | 0 | 0 | 0 |
| Alopecia | 0 | 0 | 0 | 0 | 0 | 0 | 0 | 0 | 0 | 0 | 0 | 0 |
| Urticaria | 0 | 0 | 0 | 0 | 0 | 0 | 0 | 0 | 0 | 0 | 0 | 0 |
| Abdominal pain | 0 | 0 | 0 | 0 | 0 | 0 | 0 | 0 | 0 | 0 | 0 | 0 |

National Cancer Institute Common Terminology Criteria for Adverse Events version 4.0 was applied to evaluate toxicity.

determined as 65 mg/m$^2$, which is the maximum dose for DDP-H-TAC monotherapy.

### Pharmacokinetics of platinum

To examine whether additional miriplatin following DDP-H administration further increases plasma platinum concentration, plasma samples were collected for pharmacokinetic studies from all nine patients at appropriate time periods after the administration of these agents. Since total platinum concentration in peripheral plasma during and after TAC in a control case, using 50 mg/m$^2$ of CDDP administered through the hepatic artery, peaked at the end of TAC and gradually decreased over the following 2 days (Figure 1), the plasma platinum concentration was evaluated at the end of DDP-H-TAC and miriplatin-TOCE and 24 h and 7 days after the initiation of DDP-H-TAC. At the end of DDP-H-TAC, median Cmax for level 1, 2 and 3 groups was 2000, 2933 and 4233 ng/ml, respectively. No further increase was detected following the administration of miriplatin: the plasma platinum concentration gradually decreased over 7 days to 310, 456 and 580 ng/ml in level 1, 2 and 3 groups, respectively. These results indicate that the concentration of platinum in the plasma showed no substantial increase with the addition of miriplatin to CDDP administration, as expected.

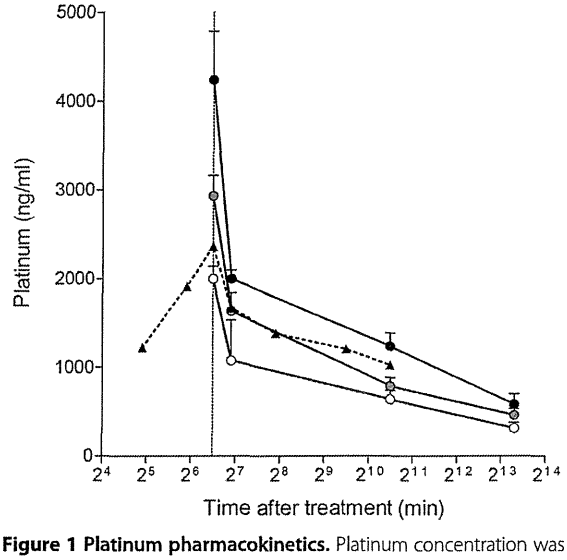


**Figure 1 Platinum pharmacokinetics.** Platinum concentration was measured in all patients at three levels. Level 1, white circle; level 2, grey circle and level 3, black circle. Plasma platinum concentration was also measured in a 63-year-old male patient during and after administration of CDDP (50 mg/m$^2$ or 80 mg/body weight) for HCCs through the proper hepatic artery at a concentration of 0.5 mg/ml and at a flow rate of 1 mg/min (black triangle with broken line).

### Anti-tumour effects

Relatively good tumour control was recorded in one patient (case 3 in the level 1 group) who underwent RFA before response evaluation. Therefore, anti-tumour response was assessed in eight patients using computed tomography (CT) and tumour markers. Changes in the HCC diameter and levels of α-fetoprotein (AFP) and des-γ-carboxy prothrombin (DCP) following treatment are summarised in Table 3 and Figure 2. With a median follow-up period of 120, 87 and 83 days for level 1, 2 and 3 groups, respectively, case 9 in the level 3 group showed a partial response (PR) to therapy. Cases 1, 4, 6 and 8 showed stable disease response, while cases 2, 5 and 7 showed progressive disease response (Table 3). These changes were consistent with the changes recorded by the tumour markers (Figure 2). One patient (case 9) with multiple HCC in both lobes (Figure 3a–d), who showed resistance to previous treatment with DDP-H-TAC and epirubicin-TACE, evidenced a PR response following combination therapy of 65 mg/m$^2$ of DDP-H-TAC and miriplatin-TOCE (Figure 3e–h). Significant reduction in HCC size in the right lobe was seen on right hepatic angiography (Figure 3a, e). A representative tumour in S6 showed no enhancement by CT during arterial portography (white arrow in Figure 3b), and significant enhancement in the early phase of CT hepatic arteriography was followed by 'corona-like' staining, which is a typical enhancement pattern seen in classical HCC (white arrowheads in Figure 3c, d) before treatment. Two months following treatment, the remaining lipiodol (black arrow in Figure 3f) and a marked decrease in tumour enhancement in the area were seen (Figure 3g, h).

## Discussion

Treatment for HCC was determined along with tumour stage and hepatic functional reserve, with only 30% of HCC cases being an indication of curative therapies

**Table 3 Anti-tumour effects: clinical efficacy**

| Antitumor response | Level 1 | Level 2 | Level 3 |
|---|---|---|---|
| | n, (Case number) | | |
| CR | 0 | 0 | 0 |
| PR | 0 | 0 | 1, (Case 9) |
| SD | 1, (Case 1) | 2, (Case 4, 6) | 1, (Case 8) |
| PD | 1, (Case 2) | 1 (Case 5) | 1, (Case 7) |
| Not evaluable | 1, (Case 3) | 0 | 0 |
| DCR (%) | 50 | 66.7 | 66.7 |
| Period of follow up (day) | | | |
| Median | 120 | 87 | 83 |
| Range | 50-213 | 24-140 | 54-84 |

Modified Response Evaluation Criteria In Solid Tumors guidelines were followed to evaluate anti-tumour effects. CR, complete response; PR, partial response; SD, stable disease; PD, progressive disease; DCR, disease control rate.

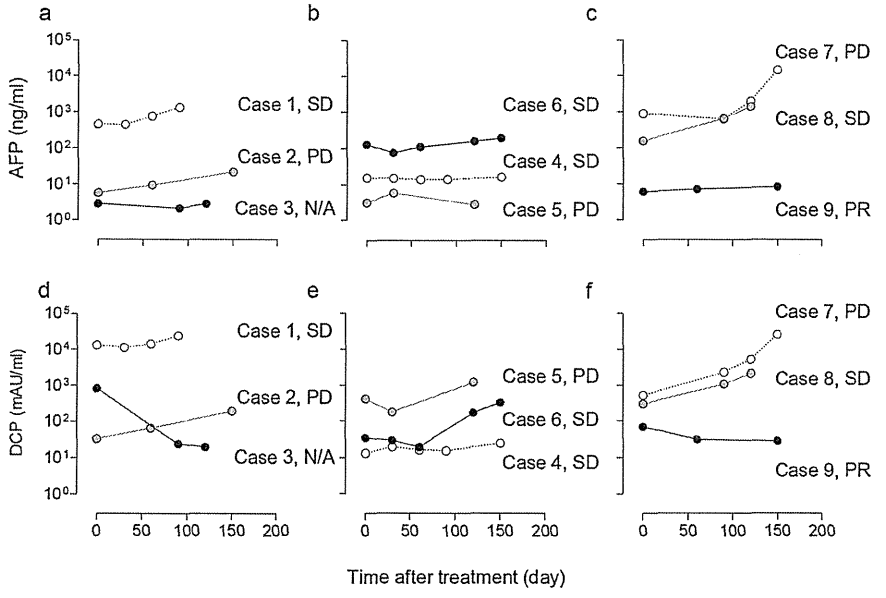


**Figure 2 Anti-tumour effects: levels of tumour markers.** Time-dependent levels of α-fetoprotein (**a–c**) and des-γ-carboxy prothrombin (**d–f**) after combination therapy of IA-call® and miriplatin at levels 1 (**a**, **d**), 2 (**b**, **e**) and 3 (**c**, **f**). Tumour markers are represented as white circles in cases 1, 4 and 7; grey circles in cases 2, 5 and 8 and black circles in cases 3, 6 and 9. PR, partial response; SD, stable disease; PD, progressive disease; N/A, not applicable for the response evaluation.

such as surgical resection and RFA [2,6]. TACE and sorafenib have recently been reported to show a definite survival advantage in advanced cases [3,4,6-8,28]. Unfortunately, however, the application of TACE or sorafenib is strictly restricted by other factors, mainly hepatic functional reserve. TACE requires a Child–Pugh score of 5–9, grade A–B, for hepatic function as it involves arterial embolization and may not be completed in a patient with major arterioportal shunts or portal vein tumour thrombosis. Sorafenib is contraindicated in patients with the exceptions of Child–Pugh score of 5–6, grade A or with brain metastases [2]. In contrast, TOCE and TAC can be provided over a broad range of cases as these are performed without arterial embolization and their efficacy has been reported [5,13-15,26]. Among various chemotherapeutic agents such as epirubicin [15] and mitomycin C [5], which carry a 15%–20% response rate, platinum agents appear to be the most promising as CDDP-TAC achieved a response rate of 33.8% in a multicentre phase II study enrolling unresectable HCC cases [13]. To investigate the highly effective and less toxic combination of TOCE and TAC, this study focused on safety issues associated with the concomitant use of two platinum agents.

Miriplatin is a third-generation platinum agent with amphipathic properties that forms a stable suspension with lipiodol and gradually releases active derivatives *in situ*, which circumvents systematic release and toxicity [18]. Treatment in few HCC cases has shown cross-resistance with different generations of platinum agents [16,21,29]. In a rat model, miriplatin exhibited higher anti-tumour activity and lower hepatic toxicity than CDDP-lipiodol [16], and promising results have been reported in HCC patients [22-24]. On the other hand, clearance of platinum compounds following short-term intravenous infusion of cisplatin was reported as triphasic (distribution half-life, 13 min; elimination half-life, 43 min and terminal half-life, 5.4 days). The short distribution half-life suggests that TAC easily exceeds tissue distribution speed and saturates the target liver on the basis of concentration rather than the total amount of the drug administered. Accordingly, DDP-H is currently the most suitable form of platinum agent for TAC by providing the highest concentration available. The combination of DDP-H-TAC and miriplatin-TOCE supports the hypothesis that higher the free platinum concentration in the target liver, lesser the systemic spill over and more sustained delivery achieved by a less cross-resistant agent leads to marked tumour response and less toxicity (both systemic and hepatic), leading to improvement in survival rates.

## Conclusions

In conclusion, in this study, no DLT was recorded following the combined administration of DDP-H and miriplatin at a maximum dose of 65 mg/m$^2$ and 120 mg/body, respectively. These are the maximum doses recommended for each monotherapy individually, indicating that the MTD